Obliquely Propagating Solitary Waves in a Four-component Magnetized Dusty Plasma

T. Akhter[1], M. M. Hossain and A. A. Mamun
Department of Physics, Jahangirnagar University, Savar, Dhaka-1342, Bangladesh

A precise theoretical investigation has been made of electrostatic solitary structures in a magnetized dusty plasma, which consists of non-inertial electron and ion fluids, and inertial negatively as well as positively charged dust fluids. The reductive perturbation method has been employed to derive the Korteweg de-Vries (K-dV) equation which admits a SW solution for small but finite amplitude limit. It has been shown that the basic features (speed, height, thickness, etc.) of such DA solitary structures are significantly modified by positive dust component and obliqueness of external magnetic field. The effects of obliqueness and external magnetic field on the nature of these compressive and rarefactive SWs are also discussed. The implications of our results in space and laboratory dusty plasmas are briefly discussed.

1. Introduction

There has been a great deal of interest in understanding linear and nonlinear features of the novel dust-acoustic (DA) waves [1], not only because they exist in both space and laboratory dusty plasmas [2,3], but also because they triggered a number of remarkable laboratory experiments [4-8]. Rao et al. [1] have first theoretically predicted the existence of this novel extremely low phase velocity (in comparison with the electron and ion thermal velocities) DA waves, where the dust mass provides the inertia and the electron and ion thermal pressures give rise to the restoring force. The prediction of Rao [1] has then conclusively been verified by a number of laboratory experiments [4-6]. The linear features of these novel DA waves have also been extensively studied for some other situations [9-11].

Rao et al., in their seminal work [1], have also studied small, but finite amplitude DA solitary waves (SWs). Mamun et al. [12] and Mamun [13] have then generalized the work of Rao et al. [1] to study arbitrary amplitude SWs. The nonlinear DA waves have also been rigorously investigated by many authors for different dusty plasma situations theoretically [14-20] as well as experimentally [7,8] during past two decades. However, all of these works on nonlinear DA waves [1,12-20] are based on the most commonly used dusty plasma model that assumes negatively charged dust. The consideration of negatively charged dust is due to the fact that in low-temperature laboratory plasmas, collection of plasma particles (viz. electrons and ions) is the only important charging process, and the thermal speeds of electrons far exceeds that of ions. But, there are some other more important charging processes by which dust grains become positively charged [21-24]. The principal mechanisms by which dust grains become positively charged are photoemission in the presence of a flux of ultraviolet photons [21,22], thermionic emission induced by the radiative heating [24], secondary emission of electrons from the surface of the dust grains [23], etc.

There is direct evidence of the coexistence of positively and negatively charged dust in different regions of space, viz. Earth's mesosphere [25], cometary tails [26,27], Jupiter's magnetosphere [26,28], etc. Chow et al. [23] have theoretically shown that due to the size effect on secondary emission, insulating dust grains with different sizes can have the opposite polarity, smaller ones being positive and larger ones being negative. The opposite situation, i.e., larger (massive) ones being positive and smaller (lighter) ones being negative, is also possible by triboelectric charging [29,30]. The coexistence of positively and negatively charged dust, with larger (massive) dust being positive and smaller (lighter) dust being negative [31-33] or vice versa [34], is also observed in laboratory devices [31-34] where dust of polymer materials are used. It may be noted here that the coexistence of same sized dust of opposite polarity may also occur by photoemission if the photoemission yields of the dust-material are very different [35].

Recently, motivated by these theoretical pre-

[1] tahminaakhter84@yahoo.com

dictions and satellite/experimental observations, a number of authors [36,37] have considered a dusty plasma with dust of opposite polarity, and have investigated linear [38] and nonlinear [37,39] DA waves. However, all of these studies [37,39,40] are limited to unmagnetized situations and the effects of the external magnetic field have not been considered in all of the previous works. Therefore, in our present work, we consider a more general, more realistic, and consistent magnetized dusty plasma system (containing non-inertial electron and ion fluids, and inertial negatively as well as positively charged dust fluids, and investigate the basic properties of finite amplitude DA SWs by the reductive perturbation method [42].

The paper is organized as follows. The basic equations governing the dusty plasma system under consideration are given in Sec. 2. The Korteweg-de Vries (K-dV) equation is derived in Sec. 3. The numerical analysis is examined in Sec. 4. A brief discussion is presented in Sec. 5.

2. Governing Equations

We consider a magnetized four-component dusty plasma system consisting of negatively charged dust, positively charged dust, Maxwellian electrons and Maxwellian ions in the presence of an external static magnetic field $\mathbf{B}_0 = B_0\hat{\mathbf{z}}$ (where $\hat{\mathbf{z}}$ is unit vector along the $z-$direction). We assume that the negative dust grains are much more massive than the positive ones. This model is relevant to dusty plasmas in cometary tails [26], upper mesosphere [25], and Jupiter's magnetosphere [26,28], where dust is charged by the secondary emission or photoemission or thermionic emission, and the dust size effect on the latter is important. Thus, at equilibrium we have $Z_p n_{p0} + Z_i n_{i0} = n_{e0} + Z_n n_{n0}$. The dynamics of the three dimensional DA waves in such a dusty plasma system is governed by

$$\frac{\partial n_s}{\partial t} + \nabla \cdot (n_s \mathbf{u}_s) = 0, \tag{1}$$

$$\frac{\partial \mathbf{u}_n}{\partial t} + (\mathbf{u}_n \cdot \nabla)\mathbf{u}_n = \nabla\psi - \omega_{cd}(\mathbf{u}_n \times \hat{\mathbf{z}}), \tag{2}$$

$$\frac{\partial \mathbf{u}_p}{\partial t} + (\mathbf{u}_p \cdot \nabla)\mathbf{u}_p = -\mu\nabla\psi + \mu\omega_{cd}(\mathbf{u}_p \times \hat{\mathbf{z}}), \tag{3}$$

$$\nabla^2\psi = [n_n - \mu_p n_p - \mu_i e^{-\psi} + \mu_e e^{\sigma\psi}] \tag{4}$$

Where, n_n (n_p) is the negative (positive) dust number density normalized by its equilibrium value n_{n0} (n_{p0}), u_s is the fluid speed of species 's' (n_n, n_p, i, e) normalized by dust-acoustic speed $C_{dn} = (Z_n K_B T_i/m_n)^{1/2}$ with m_n being the negative-dust rest mass and $Z_n K_B T_i$ is the thermal energy, ψ is the electrostatic wave potential normalized by $K_B T_i/e$ with e being the magnitude of the charge of an electron. The time variable is normalized by the ion plasma period $\omega_{pn}^{-1} = (m_n/4\pi Z_n^2 n_{n0} e^2)^{1/2}$, the space variable is normalized by the Debye radius $\lambda_{Dm} = (Z_n K_B T_i/4\pi Z_n^2 n_{n0} e^2)^{1/2}$, $\sigma = T_e/T_i$, $\mu = Z_p m_n/Z_n m_p$, $\mu_e = n_{e0}/Z_n n_{n0}$, $\mu_i = n_{i0}/Z_n n_{n0}$, and $\mu_p (= Z_p n_{p0}/Z_n n_{n0}) = 1 + \mu_e - \mu_i$. Z_n (Z_p) is the number of electrons (protons) residing on a negative (positive) dust and $\omega_{cd} = (Z_n e B_0/m_n)/\omega_{pn}$, is the dust cyclotron frequency normalized to ω_{pn}.

3. Derivation of K-dV Equation

We first investigate the basic features of the small amplitude electrostatic SWs by the reductive perturbation technique, and the stretched coordinates [42,43]:

$$\xi = \epsilon^{1/2}(l_x x + l_y y + l_z z - V_p t),$$
$$\tau = \epsilon^{3/2} t$$

Where, ϵ is a smallness parameter ($0 < \epsilon < 1$) measuring the weakness of the dispersion, and V_p (normalized by C_{dn}) is the phase speed of the perturbation mode; l_x, l_y, and l_z are directional cosines of wave vector $\mathbf{k}$ along $x-$, $y-$, and $z-$axes respectively, so that $l_x^2 + l_y^2 + l_z^2 = 1$. We can expand the perturbed quantities n_s, u_{sz}, and ψ about their equilibrium values in power of ϵ by following Refs. [44] and [42]. To obtain the x- and y-components of dust electric field and polarization drifts, we can expand the perturbed quantities $u_{x,y}$ by following a standard technique [44] where the terms of $\epsilon^{3/2}$ are included. Thus, we can expand n_s, u_{sx}, u_{sy}, u_{sz}, and ψ as

$$\left.\begin{aligned} n_s &= 1 + \epsilon n_s^{(1)} + \epsilon^2 n_s^{(2)} + \epsilon^3 n_s^{(3)} \cdots, \\ u_{sx} &= \epsilon^{3/2} u_{sx}^{(1)} + \epsilon^2 u_{sx}^{(2)} + \epsilon^{5/2} u_{sx}^{(3)} \cdots, \\ u_{sy} &= \epsilon^{3/2} u_{sy}^{(1)} + \epsilon^2 u_{sy}^{(2)} + \epsilon^{5/2} u_{sy}^{(3)} \cdots, \\ u_{sz} &= \epsilon u_{sz}^{(1)} + \epsilon^2 u_{sz}^{(2)} + \epsilon^3 u_{sz}^{(3)} \cdots\cdots, \\ \psi &= \epsilon\psi^{(1)} + \epsilon^2\psi^{(2)} + \epsilon^3\psi^{(3)} \cdots\cdots \end{aligned}\right\} \tag{5}$$

Now, expressing Eqns. (1)-(4) in terms of ξ and τ, and substituting Eqn. (5) into the resulting equations (Eqns. (1)-(4) expressed in terms of ξ and τ),

one can easily develop different sets of equations in various powers of ϵ. To the lowest order in ϵ one obtains

$$n_e^{(1)} = \frac{\psi^{(1)}}{\sigma}, \qquad n_i^{(1)} = -\frac{\psi^{(1)}}{\gamma}, \tag{6}$$

$$n_n^{(1)} = -\frac{l_z^2}{V_p^2}\psi^{(1)}, \quad n_p^{(1)} = \frac{\mu l_z^2}{V_p^2} l_z^2 \psi^{(1)}, \tag{7}$$

$$u_{nz}^{(1)} = -\frac{l_z}{V_p}\psi^{(1)}, \quad u_{pz}^{(1)} = -\frac{\mu l_z}{V_p}\psi^{(1)}, \tag{8}$$

$$n_n^{(1)} - \mu_p n_p^{(1)} + \mu_i \psi^{(1)} + \mu_e \sigma \psi^{(1)} = 0 \tag{9}$$

Using Eqns. (6)-(8) into Eqn. (9), we get the linear dispersion relation for the DA waves modified by the presence of the moving dust of opposite polarity.

$$V_p = \sqrt{\frac{(1+\mu_p\mu)l_z^2}{(\mu_i + \mu_e/\sigma)}} \tag{10}$$

The x- and y-components of the electric-field drift are

$$u_{nx}^{(1)} = u_{px}^{(1)} = -\frac{l_y}{\omega_{cd}}\frac{\partial \psi^{(1)}}{\partial \xi}, \tag{11}$$

$$u_{ny}^{(1)} = u_{py}^{(1)} = \frac{l_x}{\omega_{cd}}\frac{\partial \psi^{(1)}}{\partial \xi} \tag{12}$$

Taking the next higher order co-efficient of ϵ, one obtains

$$u_{nx}^{(2)} = -\frac{l_x V_p}{\omega_{cd}^2}\frac{\partial^2 \psi^{(1)}}{\partial \xi^2}, \quad u_{ny}^{(2)} = -\frac{l_y V_p}{\omega_{cd}^2}\frac{\partial^2 \psi^{(1)}}{\partial \xi^2} \tag{13}$$

$$u_{px}^{(2)} = \frac{l_x V_p}{\mu\omega_{cd}^2}\frac{\partial^2 \psi^{(1)}}{\partial \xi^2}, \quad u_{py}^{(2)} = \frac{V_p}{\mu\omega_{cd}^2}\frac{\partial^2 \psi^{(1)}}{\partial \xi^2}, \tag{14}$$

$$\frac{\partial^2 \psi^{(1)}}{\partial \xi^2} = n_n^{(2)} - \mu_p n_p^{(2)} - \mu_i[\frac{1}{2}\psi(1)^2 - \psi(2)] + \mu_e[\sigma\psi(1) + \frac{1}{2}\sigma^2\psi(1)^2] \tag{15}$$

Again, following the same procedure one can obtain the next higher order continuity equations, and z-component of momentum equations as

$$\frac{\partial n_s^{(1)}}{\partial \tau} - V_p\frac{\partial n_s^{(2)}}{\partial \xi} + l_x\frac{\partial u_{sx}^{(2)}}{\partial \xi} + l_y\frac{\partial u_{sy}^{(2)}}{\partial \xi} + l_z\frac{\partial u_{sz}^{(2)}}{\partial \xi} + l_z\frac{\partial}{\partial \xi}[n_s^{(1)}u_{sz}^{(1)}] = 0, \tag{16}$$

$$\frac{\partial u_{nz}^{(1)}}{\partial \tau} - V_p\frac{\partial u_{nz}^{(2)}}{\partial \xi} + l_z u_{nz}^{(1)}\frac{\partial u_{nz}^{(1)}}{\partial \xi} = l_z\frac{\partial \psi^{(2)}}{\partial \xi}, \tag{17}$$

$$\frac{\partial u_{pz}^{(1)}}{\partial \tau} - V_p\frac{\partial u_{pz}^{(2)}}{\partial \xi} + l_z u_{pz}^{(1)}\frac{\partial u_{pz}^{(1)}}{\partial \xi} = -\mu l_z\frac{\partial \psi^{(2)}}{\partial \xi} \tag{18}$$

Now, using Eqns. (6)-(18), we can eliminate $n_p^{(2)}$, $n_n^{(2)}$, and $\psi^{(2)}$ and can finally obtain

$$\frac{\partial \Phi}{\partial \tau} + A\Phi\frac{\partial \Phi}{\partial \xi} + B\frac{\partial^3 \Phi}{\partial \xi^3} = 0 \tag{19}$$

Where, $\Phi = \psi^{(1)}$. This is the K-dV equation with the coefficients A and B of nonlinear and dispersive terms, are given by

$$A = k[\frac{\mu_p\mu^2 l_z^4}{V_p^4} - \frac{3l_z^4}{V_p^4} + 2\mu_i - \frac{2\mu_e}{\sigma^2}], \tag{20}$$

$$B = k[1 + (1 - l_z^2)(\frac{1}{\omega_{cd}^2} + \frac{1}{\mu^2\omega_{cd}^2})] \tag{21}$$

Where, $k = \frac{V_p^3}{2l_z^2(1+\mu_p\mu)}$.

The general expressions for the coefficients A and B (by using (20) and (21)) are used to have some numerical appreciations of our results, viz. the SW height and width are numerically analyzed.

It is clear from Eqns. (19)-(21) that the solitary potential profile is positive (negative) if $A > 0$ ($A < 0$). Therefore, $A(\mu = \mu_c) = 0$, where μ_c is the critical value of μ above (below) which the SWs with a positive (negative) potential exists gives the value of μ_c. As μ_p (positive dust) increases, we need a higher value of μ, i.e., more negative dust, in order for rarefactive SWs to exist (Fig. 1). Apparently the parameter regimes are divided into two regions one for compressive solitons and other for rarefactive solitons. It may be noted that from Eqns. (19) and (21) that the coefficient A of the nonlinearity remains positive for the positive solitary potential profile and correspondingly compressive solitons exist in the given plasma system. However, introduction of magnetic field leads to the appearance of compressive and rarefactive solitons.

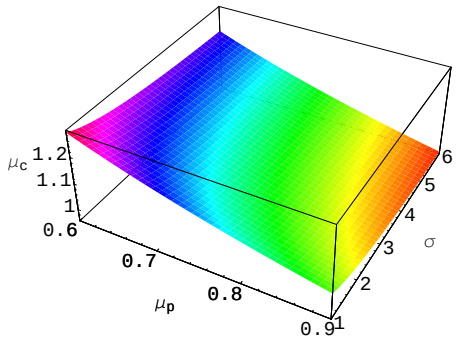

FIG. 1: Variation of μ_c(critical value of μ) with μ_p and σ for $\mu_e = 5$.

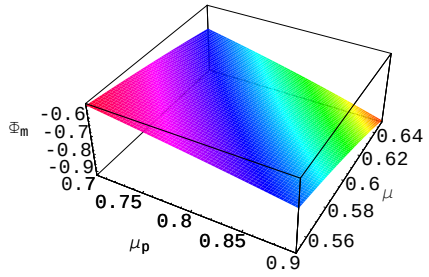

FIG. 2: The variation of Φ_0 (height of negative SW) with μ_p and μ for $\sigma = 5$, $U_0 = 0.4$, $\delta = 10^\circ$ and $\mu_e = 10$.

4. Numerical Analysis

The steady-state solution of this K-dV equation (19) is obtained by transforming the independent variables to $\zeta = \xi - U_0\tau'$ and $\tau' = \tau$, where U_0 is the speed of the SWs, and imposing the appropriate boundary conditions, viz. $\Phi \to 0$, $d\Phi/d\zeta \to 0$, $d^2\Phi/d\zeta^2 \to 0$ at $\zeta \to \pm\infty$. Thus, one can express the stationary solitary wave (SW) solution of the K-dV Eqn. (19) as

$$\Phi = \Phi_0 \mathrm{sech}^2\left(\frac{\zeta}{\Delta}\right) \tag{22}$$

Where, the amplitude Φ_0, and the width Δ are given by

$$\Phi_0 = \frac{3U_0}{A}, \tag{23}$$

$$\Delta = \sqrt{\frac{4B}{U_0}} \tag{24}$$

The general expressions for the coefficients A and B (by using (20) and (21)) are used to have some numerical appreciations of our results, viz. the solitary wave height and width are numerically analyzed.

It is obvious from Eqns. (23) and (24) that as U_0 increases, the amplitude (width) of the SWs increases (decreases). It also has been shown graphically that how the amplitude and the width of the positive and negative solitary potential profiles vary with μ_p, μ, μ_e, σ, δ, and ω_{cd}. These are displayed in Figs. 2-10. From Fig. 2, one can observe that the magnitude of the amplitude of the negative solitary profiles increases with μ_p and μ. The width of the negative solitary profiles

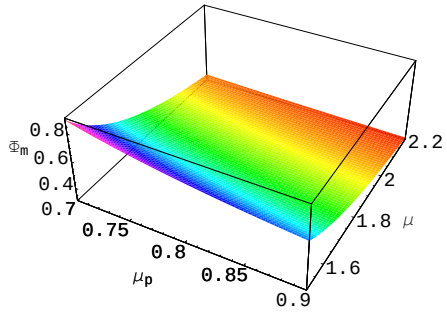

FIG. 3: Showing how Φ_0 (height of positive SW) depends on μ_p and μ for $U_0 = 0.4$, $\sigma = 5$, $\mu_e = 10$, and $\delta = 10^\circ$.

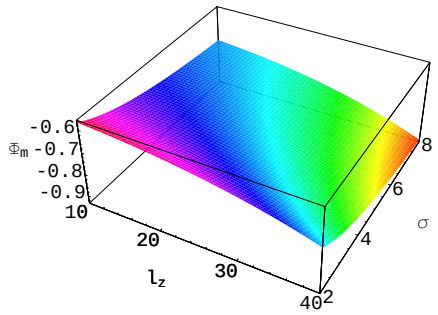

FIG. 4: Showing how Φ_0 (height of negative SW) depends on l_z and σ for $U_0 = 0.4$, $\mu_p = 0.8$, $\mu = 0.6$, and $\mu_e = 10$.

increases with μ_p and decreases with μ (as shown in Fig. 6). One can observe that the magnitude of the amplitude (width) of the positive solitary profiles decreases (increases) with μ_p and μ (as shown in Figs. 3 and 7). On the other hand, it is clear from Figs. 4 and 8 that the magnitude of the am-

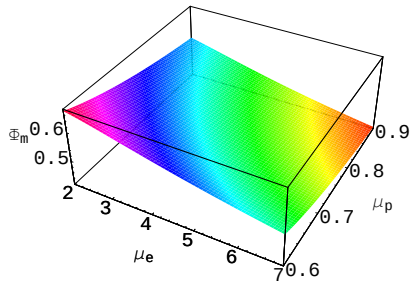

FIG. 5: Showing how Φ_0 (height of positive SW) depends on μ_e and μ_p for $U_0 = 0.4$, $\sigma = 5$, $\mu = 2$, and $\delta = 10^\circ$.

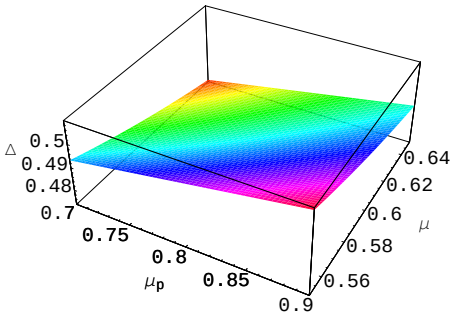

FIG. 6: The variation of Δ (thickness of negative SW) with μ_p and μ for $\sigma = 5$, $U_0 = 0.4$, $\delta = 10^\circ$ and $\mu_e = 10$.

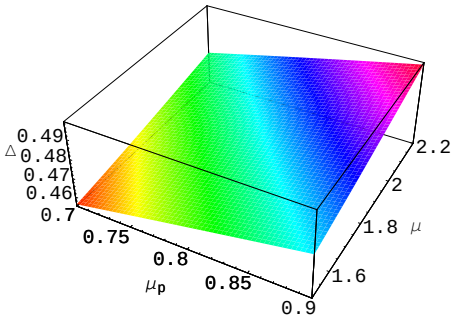

FIG. 7: Showing how Δ (thickness of positive SW) depends on μ_p and μ for $U_0 = 0.4$, $\sigma = 5$, $\mu_e = 10$, and $\delta = 10^\circ$.

plitude of the negative solitary profiles and their width increase with both l_z and σ. From Fig. 5, one can observe that the magnitude of the amplitude of the negative solitary profiles decreases with μ_e and μ_P. The width of the negative solitary profiles increases with μ_e and decreases with μ_P (as

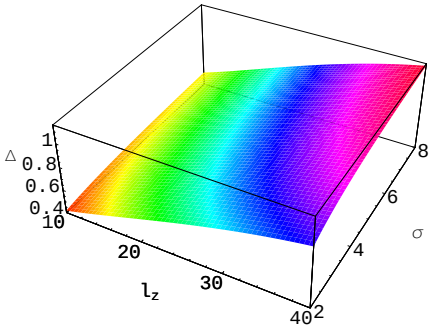

FIG. 8: Showing how Δ (thickness of negative SW) depends on l_z and σ for $U_0 = 0.4$, $\mu_p = 0.8$, $\mu = 0.6$, and $\mu_e = 10$.

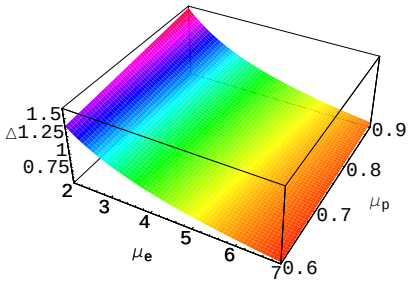

FIG. 9: Showing how Δ (thickness of positive SW) depends on μ_e and μ_p for $U_0 = 0.4$, $\sigma = 5$, $\mu = 2$, and $\delta = 10^\circ$.

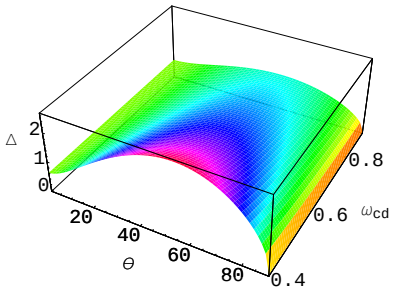

FIG. 10: Showing how Δ (thickness of negative SW) depends on θ and ω_{cd} for $U_0 = 0.4$, $\sigma = 5$, $\mu_e = 5$, $\mu_p = 0.8$ and $\mu = 0.4$.

shown in Fig. 9). Fig. 10 shows that the width of the solitary profile increases with δ for the lower range (i.e., from 0° to 45°), but decreases for its higher range (i.e., from 45° to 90°).

5. Discussion

The basic features of the DA SWs in a magnetized dusty plasma containing warm adiabatic positive as well as negative dust, adiabatic electrons and adiabatic ions, are investigated theoretically. By employing the Reductive perturbation technique, we have derived K-dV equation. The results, which have been found from this investigation, can be summarized as follows.

The width of positive and negative SWs increases with the increase of l_z, σ, and μ_p, but decreases with the increase of U_0, μ, and μ_e. The basic properties (polarity, speed, amplitude and width) of the DA SWs are found to be significantly modified by the presence of opposite polarity dust in presence of external magnetic field. The existence of the positive and negative solitary potential structures is due to the presence of the opposite polarity dust component, which is allowed under some parametric conditions. It is obvious that the amplitude of both the compressive and rarefactive SWs decreases with the rise of l_z ($l_z = \cos\theta$, with θ the angle between the directions of the wave propagation vector $\mathbf{k}$ and the external magnetic field B_0). Fig. 10 shows how the width (Δ) of these SWs changes with the obliqueness (θ) and the magnitude of the external magnetic field (ω_{cd}). It is observed that the width (Δ) increases with θ for its lower range (i.e., from 0° to 45°), but decreases for its higher range (i.e., from 45° to 90°). Though in Fig. 10 the variation of Δ with θ has been shown for any value of θ between 0° and 90°, our perturbation method, which is only valid for small but finite amplitude limit, is not valid for large θ, which makes the wave amplitude large. It is seen that the magnitude of the external magnetic field has no effect on the amplitude of the SWs. However, it does have an effect on the width of these SWs. It is shown that, as we increase the magnitude of the magnetic field, the width of these SWs decreases, i.e., the external magnetic field makes the solitary structures more spiky.

We have used a wide range of the dusty plasma parameters (viz. $\mu = 0.1 - 5$, $\mu_e = 0.2 - 10$, $\mu_p = 0.2 - 0.9$, $\theta = 0° - 90°$, $\sigma = 1 - 15$, and $\omega_{cd} = 0.1 - 0.9$) in our numerical analysis. The values of the dusty plasma parameters, for which the existence of the SWs is found, are also within the ranges of the dusty plasma parameters corresponding to dust-plasma parameters for both space environments [25-28], and laboratory devices [31-34].

It may be stressed here that the results of this investigation should be useful in understanding the nonlinear features of the localized electrostatic disturbances in mesospheric plasmas, in which positively and negatively charged dust particles, free electrons, and ions are the plasma species. The present investigation may be useful not only in diagnosing the temporal behavior of polar mesospheric summer echoes during active modification [45] but also in analyzing the stability of the mesospheric plasma layer [46] and the formation and evolution of polar mesospheric clouds [47]. It is important to mention here that solitary negative (positive) potential may trap positively (negatively) charged dust particles, which, in turn, attract dust particles of opposite polarities to form larger sized dust particles or to be coagulated into extremely large sized neutral dust in cometary tails [26,27], in upper mesosphere [25,46-48], in Jupiter's magnetosphere [26,28] or even in laboratory experiments. Thus, the results of the present investigation should help to identify the origin of charge separation as well as dust coagulation in mesospheric plasma containing positive and negative dust particles [25,45,47]. It may be added here that, in our present work, we have neglected the effects of strong correlation among charged dust [3] and dust neutral collisions [49,50] etc.

To conclude, it may be added that the time evolution and stability analysis of these solitary structures are also problems of great importance but beyond the scope of the present work.

References

[1] N. N. Rao, P. K. Shukla and M. Y. Yu, Planet. Space Sci. **38**, 543 (1990).

[2] F. Verheest, (Kluwer Academic Publishers, Dordrecht, 2000).

[3] P. K. Shukla and A. A. Mamun, (IOP Publishing Ltd., Bristol, 2002).

[4] A. Barkan, R. L. Merlino and N. D'Angelo, Phys. Plasmas **2**, 3563 (1995).

[5] C. Thompson et al., Phys. Plasmas **4**, 2331 (1997).

[6] R. L. Merlino and J. Goree, Phys. Today **57**(7), 32 (2004).

[7] P. Bandyopadhyay et al., Phys. Rev. Lett. **101**, 065006 (2008).

[8] J. Heinrich, S. H. Kim and R. L. Merlino, Phys. Rev. Lett. **103**, 115002 (2009).

[9] R. K. Varma, P. K. Shukla and V. Krishan, Phys. Rev. E **47**, 3612 (1993).

[10] F. Melandsø, Phys. Plasmas **3**, 3890 (1996).

[11] P. K. Kaw and A. Sen, Phys. Plasmas **5**, 3552 (1998).
[12] A. A. Mamun, R. A. Cairns and P. K. Shukla, Phys. Plasmas **3**, 702 (1996).
[13] A. A. Mamun, Astrophys. Space Sci. **268**, 443 (1999).
[14] P. K. Shukla and A. A. Mamun, IEEE Trans. Plasma Sci. **29**, 221 (2001).
[15] A. A. Mamun and P. K. Shukla, Phys. Lett. A **290**, 173 (2001).
[16] A. A. Mamun and P. K. Shukla, Europhys. Lett. **87**, 25001 (2009).
[17] A. A. Mamun and P. K. Shukla, New J. Phys. **11**, 103022 (2009).
[18] K. S. Ashrafi, A. A. Mamun and P. K. Shukla, Europhys. Lett. **92**, 15004 (2010).
[19] H. Alinejad and A. A. Mamun, Phys. Plasmas **17**, 123706 (2010).
[20] M. Tribeche and A. Merriche, Phys. Plasmas **18**, 034502 (2011).
[21] M. Rosenberg and D. A. Mendis, IEEE Trans. Plasma Sci. **23**, 177 (1995).
[22] V. E. Fortov et al., JETP **87**, 1087 (1998).
[23] V. W. Chow, D. A. Mendis and M. Rosenberg, J. Geophys. Res. **98**, 19065 (1993).
[24] M. Rosenberg, D. A. Mendis and D. P. Sheehan, IEEE Trans. Plasma Sci. **27**, 239 (1999).
[25] O. Havnes et al., J. Geophys. Res. **101**, 10839 (1996).
[26] M. Horányi, Annu. Rev. Astron. Astrophys. **34**, 383 (1996).
[27] T. A. Ellis and J. S. Neff, Icarus **91**, 280 (1991).
[28] M. Horányi, G. E. Morfill and E. Grün, Nature **363**, 144 (1993).
[29] P. K. Shukla and M. Rosenberg, Phys. Scripta **73**, 196 (2006).
[30] D. J. Lacks and A. Levandovsky, J. Electrost. **65**, 107 (2007).
[31] H. Zhao, G. S. P. Castle and I. I. Inculet, J. Electrost. **55**, 261 (2002).
[32] H. Zhao et al., IEEE Trans. Ind. Appl. **39**, 612 (2003).
[33] S. Trigwell et al., IEEE Trans. Ind. Appl. **39**, 79 (2003).
[34] F. S. Ali et al., J. Electrost. **45**, 139 (1998).
[35] D. A. Mendis and M. Rosenberg, Annu. Rev. Astron. Astrophys. **32**, 419 (1994).
[36] A. A. Mamun and P. K. Shukla, Geophys. Res. Lett. **29**, 1870 (2002).
[37] F. Verheest, Phys. Plasmas **16**, 013704 (2009).
[38] N. D'Angelo, Planet. Space Sci. **49**, 1251 (2001).
[39] P. H. Sakanaka and P. K. Shukla, Phys. Scripta **T84**, 181 (2000).
[40] F. Sayed and A. A. Mamun, Phys. Plasmas **14**, 014501 (2007).
[41] P. K. Shukla and M. Rosenberg, Phys. Plasmas **6**, 1038 (1999).
[42] H. Washimi and T. Taniuti, Phys. Rev. Lett. **17**, 996 (1966).
[43] A. A. Mamun, Phys. Scr. **57**, 258 (1998).
[44] P. K. Shukla and M. Y. Yu, J. Math. Phys. **19**, 2506 (1978).
[45] A. Mahmoudian et al., Ann. Geophys. **129**, 2169 (2011).
[46] B. P. Pandey and S. V. Vladimirov, Phys. Plasmas **18**, 122902 (2011).
[47] S. I. Popel et al., Advances in Space Research, **37**, 414 (2006).
[48] P. K. Shukla, Phys. Plasmas **11** 3676 (2004).
[49] W. M. Moslem, Phys. Plasmas **10**, 3168 (2003).
[50] Ju-Kui Xue, Phys. Rev. E **69**, 016403 (2004).

Received: 27 September, 2012
Accepted: 22 March, 2013